

SCIENTIFIC COMMUNICATIONS

RECOGNITION OF PORPHYRY QUARTZ IN STREAM SEDIMENTS BY FLUID INCLUSION PETROGRAPHY AND CATHODOLUMINESCENCE MICROSCOPY: RESULTS OF SYSTEMATIC DISPERSION STUDIES AND POTENTIAL APPLICATIONS IN PORPHYRY EXPLORATION

Mitchell M. Bennett, 1,° Thomas Monecke, 1,† T. James Reynolds, 1,2 and Nigel M. Kelly³

¹Center to Advance the Science of Exploration to Reclamation in Mining, Department of Geology and Geological Engineering, Colorado School of Mines, 1516 Illinois Street, Golden, Colorado 80401

²FLUID INC., 1401 Wewatta St. #PH3, Denver, Colorado 80202

³Bruker Nano Analytics, 5465 E. Cheryl Parkway, Madison, Wisconsin 53711

Abstract

Regional stream sediment surveys are an important exploration tool used in the search for concealed or partially concealed porphyry deposits. It is shown here that quartz contained in the coarse fraction of stream sediments can be used as an indicator mineral to supplement geochemical analyses conducted on the fine fraction, such as the measurement of the bulk cyanide leach extractable gold content. A method is proposed that allows separation of quartz grains from the coarse rejects of stream sediment samples to prepare grain mounts for petrographic analysis. Based on optical cathodoluminescence microscopy and fluid inclusion petrography, the number of porphyry quartz grains in each grain mount is then identified. Case studies conducted at Vert de Gris in Haiti and Hides Creek in Papua New Guinea show that porphyry quartz grains could be confidently identified in sediments in the catchment areas of both porphyries. Because the cost of microscopic analysis of quartz is small compared to the expense of sampling and geochemical analysis, the developed technique could be routinely used in large greenfield exploration programs. It is envisaged here that petrographic analysis of quartz grains can contribute valuable information for prioritization of targets defined based on their geochemical signatures.

Introduction

Porphyry copper deposits are the world's most important source of copper, with precious metals commonly being recovered as by-products (Sillitoe, 2010). The hypogene ores in porphyry deposits form large low-grade stockwork and disseminated sulfide zones (Nielsen, 1968; Gustafson and Hunt, 1975; Gustafson and Quiroga, 1995; Sillitoe, 2010; Monecke et al., 2018) that are spatially associated with shallow (≤1−10 km) plutonic stocks and dike swarms (Lowell and Guilbert, 1970; Gustafson and Hunt, 1975; Titley and Beane, 1981; Seedorff et al., 2005; Sillitoe, 2010) formed in suprasubduction and postsubduction settings (Richards, 2011).

Exploration for porphyry deposits is challenging, despite their large size. This is especially true in areas characterized by deep weathering and dense vegetation cover. In these environments, regional surface-geochemical surveys have proven to be powerful exploration tools, allowing detection of chemical anomalies associated with porphyry deposits. This includes bulk cyanide leach extractable gold (BLEG) analysis of the fine-grained fraction of stream sediment samples (Sillitoe and Thompson, 2006). Regional BLEG surveys have been key in the discovery of several porphyry deposits, including Batu Hijau in Indonesia (Meldrum et al., 1994), Elang in Indonesia (Maryono et al., 2018), Phu Kham in Laos (Tate, 2005), and Reko Diq in Pakistan (Perelló et al., 2008).

[†]Corresponding author: e-mail, tmonecke@mines.edu ^oCurrent address: U.S. Geological Survey, Geology, Geophysics, and Geochemistry Science Center, One Denver Federal Center, Denver, Colorado 80225. The present study tests whether quartz contained in the coarse reject fraction of regional stream sediment surveys can be used to link BLEG geochemical anomalies to the existence of a porphyry target. Quartz may be an ideal indicator mineral owing to its abundance in porphyry veins and the fact that it is highly stable during weathering, allowing transport away from the porphyry source. This contribution introduces a new method that combines optical cathodoluminescence (CL) microscopy with fluid inclusion petrography to identify porphyry quartz grains in stream sediment samples. The method was evaluated in two dispersion studies in Haiti and Papua New Guinea. These studies show that simple petrographic studies of quartz from stream sediments can add significant value to regional BLEG exploration programs.

Petrographic Characteristics of Porphyry Quartz

Reliable identification of porphyry quartz in the coarse reject fraction of BLEG stream sediment samples that returned anomalous geochemical results is only possible if certain mineral properties can be identified that are intrinsic to quartz of this origin. Although previous studies have shown that the trace element content of quartz (Suttner and Leininger, 1972; Heynke et al., 1992; Monecke et al., 2002; Götze et al., 2004; Müller et al., 2010; Rusk, 2012), the composition of fluid inclusion leachates (Bottrell et al., 1988; Yardley et al., 1993; Götze et al., 2004) or individual fluid inclusions (Heinrich et al., 1999; Pudack et al., 2009; Stefanova et al., 2014), and the stable isotopic composition of quartz (Clayton et al., 1972; Blatt, 1987; Vennemann et

al., 1992; Palmer et al., 2004) can be used to fingerprint the origin of this mineral, the analytical costs are prohibitive to allow routine use of these techniques in mineral exploration. Discrimination of porphyry quartz from other types of quartz in stream sediment samples therefore needs to be based on petrographic characteristics for reasons of practicality and cost efficiency.

Previous studies have established that different quartz vein types occur in porphyry deposits that show consistent crosscutting relationships (Nielsen, 1968; Gustafson and Hunt, 1975; Dilles and Einaudi, 1992; Gustafson and Quiroga, 1995; Monecke et al., 2018). The same sequence of veining occurs in porphyry deposits worldwide because the formation of these vein types is related to the overall cooling history of porphyry systems over time (Gustafson and Hunt, 1975; Sillitoe, 2010; Monecke et al., 2018). The CL characteristics and fluid inclusion inventory of quartz occurring in the different vein types have been studied extensively (Bodnar, 1995; Monecke et al., 2018; Sun et al., 2021; Tsuruoka et al., 2021) and can be directly linked to the pressure-temperature (P-T) conditions of quartz deposition (Fig. 1). These previous studies established that quartz formed in high-temperature (≥425°C) porphyry veins (referred to as porphyry quartz in this contribution) is typified by optical CL colors and fluid inclusion petrographic characteristics that are distinct from quartz formed in other geologic environments.

Early quartz veins in porphyry deposits, commonly referred to as A veins (Gustafson and Hunt, 1975), are volumetrically abundant and can make up more than 10% of the rock volume in the core of the deposits (Gruen et al., 2010). The veins are formed at high temperatures (≥500°C) and lithostatic pressure conditions (Monecke et al., 2018). The quartz in these veins exhibits a stable, dark-blue optical CL emission—the so-called long-lived CL signal (Götze et al., 2001)—following an initial color change during the first ~30 s of electron bombardment in hot-cathode CL instruments. The quartz may preserve oscillatory growth zoning under CL; however, in most deposits, zoning is rare because the quartz has recrystallized at high temperatures during repeated vein reopening (Monecke et al., 2018; Sun et al., 2021; Tsuruoka et al., 2021). Later high-temperature veins, referred to as B veins (Gustafson and Hunt, 1975), are characterized by center lines with euhedral quartz crystals terminating in vugs. Quartz in these veins is formed at temperatures between 425° and 500°C and pressures fluctuating between hydrostatic and lithostatic conditions (Monecke et al., 2018). The quartz shows well-developed growth zoning and exhibits a long-lived bluish purple to dark brown CL emission (Monecke et al., 2018; Sun et al., 2021; Tsuruoka et al., 2021).

The fluid inclusion characteristics of porphyry quartz depend on pressure (Fig. 1). In porphyry deposits emplaced at ~1.5 to ~4.2 km below the paleosurface, the magmatic-hydrothermal fluids forming the high-temperature vein quartz occur in the two-phase field of the H₂O-NaCl system (Bodnar, 1995; Monecke et al., 2018). Therefore, the high-temperature quartz contains abundant hypersaline liquid and vapor-rich inclusions (Reynolds and Beane, 1985; Hedenquist et al., 1998; Redmond et al., 2004; Klemm et al., 2007; Pudack et al., 2009; Landtwing et al., 2010; Stefanova et al., 2014; İmer et al., 2016; Gregory, 2017; Tsuruoka et al., 2021). At room

temperature, hypersaline liquid inclusions contain a large halite daughter crystal because the salinity of these inclusions may range up to ~70 wt % NaCl equiv (Monecke et al., 2018; Klyukin et al., 2019). Inclusions formed at such high temperatures were entrapped at lithostatic conditions (Monecke et al., 2018) and will have suffered postentrapment modification (Fig. 1) during decompression of the magmatic-hydrothermal system to hydrostatic conditions (Sun et al., 2021). However, despite textural modification, they can still be identified petrographically as hypersaline liquid or vapor-rich inclusions (Sun et al., 2021). In addition, the porphyry quartz in high-temperature veins will also contain later fluid inclusions that were entrapped in the two-phase field at hydrostatic conditions and crosscut the earlier-formed high-temperature quartz. These fluid inclusions do not show textural changes caused by postentrapment modification and can be easily identified (Fig. 1).

Porphyry quartz formed in deep (≥4.2 km below paleosurface) deposits does not contain high-salinity and vapor-rich inclusions (Redmond et al., 2004; Klemm et al., 2007; Rusk et al., 2008; Landtwing et al., 2010; Stefanova et al., 2014; Gregory, 2017). In such deep porphyry deposits, inclusions were entrapped in the single-phase field of the H₂O-NaCl system (Fig. 1). The vapor to liquid ratio of these inclusions varies with the P-T conditions of entrapment. If the inclusions have near-critical densities, they are referred to as intermediate-density inclusions, but they are difficult to identify petrographically. Vapor-like intermediate-density inclusions and vapor-rich inclusions entrapped in the two-phase field of the H₂O-NaCl system are not petrographically distinguishable (Klyukin et al., 2019). Similarly, the distinction between liquid-like intermediate-density and liquid-rich inclusions may be tenuous (Tsuruoka et al., 2021).

When considered together, the CL characteristics and fluid inclusion inventory of porphyry quartz in high-temperature veins are distinct and can be used to fingerprint the origin of quartz grains in stream sediments. Based on these parameters, different certainty levels can be assigned for a given quartz grain to have been derived from a porphyry source (Fig. 2). Quartz grains in stream sediments that show a blue to purple CL emission and contain hypersaline-liquid inclusions as well as vapor-rich inclusions must have undoubtedly derived from a porphyry source (Fig. 2). However, a porphyry source may not be entirely ascertained if only hypersaline liquid or only vapor-rich inclusions are identified in quartz grains that have a blue to purple CL color (Fig. 2). A similarly lower confidence level is assigned to quartz grains that show a long-lived blue to purple CL emission and that only contain what might be interpreted to be intermediate-density fluid inclusions (Fig. 2).

For reasons of practicability, porphyry quartz as defined in this study includes quartz phenocrysts that have been overprinted by high-temperature magmatic-hydrothermal fluids. Quartz phenocrysts also show long-lived blue CL colors (Götze et al., 2001; Augustsson and Reker, 2012; Gao et al., 2022) and may lack growth zoning (Watt et al., 1997; Götze et al., 2001; Augustsson and Reker, 2012). Without textural context, sand grains derived from phenocrysts may not be distinguishable from high-temperature vein quartz. Quartz phenocrysts hosted in mineralized porphyries can contain the same secondary fluid inclusion assemblages as high-temperature vein

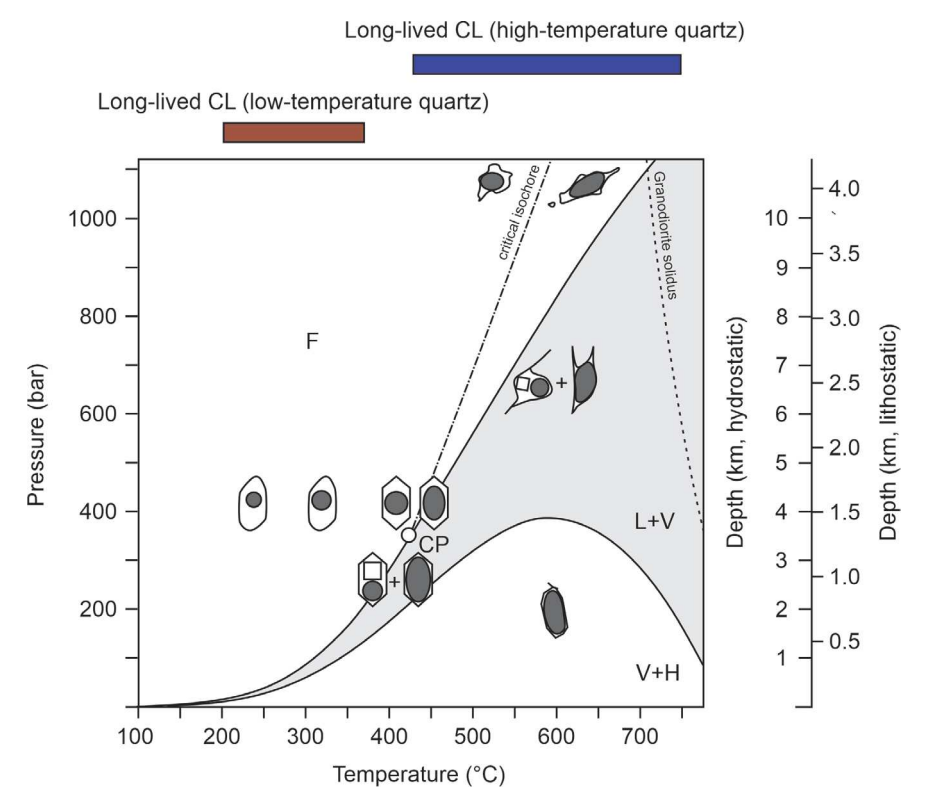


Fig. 1. Phase diagram showing the room temperature appearance of fluid inclusions in porphyry quartz veins formed at different pressure-temperature conditions. The shaded area highlights the conditions at which liquid and vapor (L + V) coexist and hypersaline liquid and vapor-rich inclusions are entrapped in porphyry quartz. The diagram shows the locations of the single-phase field (F) and the vapor plus halite (V + H) coexistence field. The shapes of fluid inclusions that have been entrapped at temperatures exceeding the brittle-ductile transition have been affected by postentrapment modification, schematically indicated as having irregular surfaces. The phase diagram is constructed for the H_2O -NaCl system at a salinity of 5 wt % NaCl equiv. The critical point (CP) for a magmatic-hydrothermal fluid of this composition is located at $422^{\circ}C$ and 337 bar. The critical isochore at which a magmatic-hydrothermal fluid with a salinity of 5 wt % NaCl has a density of 0.48 g/cm³ divides the single-phase field into regions of lower (vapor-like) and higher (liquid-like) densities. The diagram also schematically shows the temperature ranges over which different long-lived cathodoluminescence (CL) emissions occur in porphyry quartz. The granodiorite solidus is given for reference. Diagram modified from Bodnar (1995) and Monecke et al. (2018).

quartz (Hezarkhani and Williams-Jones, 1998; Ulrich et al., 2002; Pudack et al., 2009; Chang et al., 2018; Gao et al., 2022).

Veins in porphyry deposits formed at low (≤425°C) temperatures contain variable amounts of quartz. Ore-bearing veins commonly lack quartz (Fournier, 1967; Nielsen, 1968; Reynolds and Beane, 1985; Dilles and Einaudi, 1992; Gustafson and Quiroga, 1995; Stefanova et al., 2014; Monecke et al., 2018; Sun et al., 2021; Tsuruoka et al., 2021) and, therefore, do not contribute to the quartz inventory of stream sediments. Later quartz-bearing veins contain euhedral quartz that is characterized by long-lived red to brown CL colors (Monecke et al., 2018; Sun et al., 2021; Tsuruoka et al., 2021), although quartz showing a pronounced yellow CL emission during electron bombardment can also be present (Monecke et al., 2018). The low-temperature quartz-bearing veins are formed within the single-phase field of the H₂O-NaCl system and fluid inclusions entrapped under these conditions are liquid rich (Fig. 1). In some porphyry deposits, the pressure conditions are low enough to allow coexistence of liquid and vapor (Hedenquist et al., 1998; Pudack et al., 2009) resulting in entrapment of vapor-rich inclusions and liquid-rich inclusions without NaCl crystals. Fluid inclusions in the lowtemperature veins have not typically been affected by postentrapment modification (Fig. 1), because the vein quartz was formed at hydrostatic conditions. Because the quartz CL is not unique and the fluid inclusion characteristics of the quartz in the low-temperature veins are similar to quartz from other environments (Bodnar et al., 2014), quartz grains with these properties in stream sediments may not indicate the presence of an eroding porphyry deposit (Fig. 2).

Analytical Protocol

Following establishment of petrographic criteria that allow identification of porphyry quartz grains in stream sediment samples, an analytical protocol was developed to separate quartz from other minerals contained in the coarse reject fractions of BLEG stream sediments that yielded geochemically anomalous results. The analytical protocol was developed to allow processing of a large number of samples to allow the developed method to be used as an add-on to regional BLEG surveys.

Initially, the coarse rejects (>177 μ m) of geochemically anomalous BLEG samples (~500 g) were sieved to obtain the 250- to 500- μ m-size fractions for further analysis. This size fraction was then split into subsamples of ~100-g weight using a riffle splitter. One subsample was carefully washed to ensure

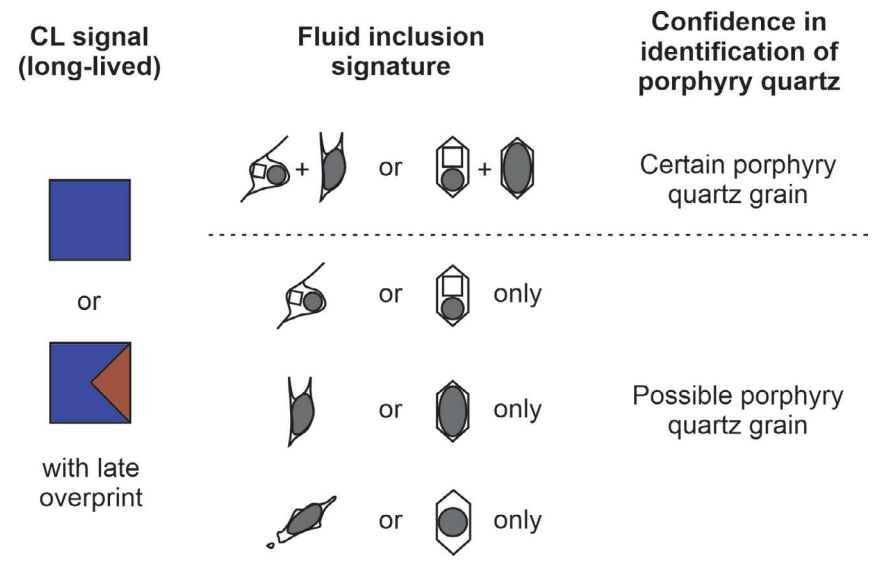


Fig. 2. Diagram establishing confidence in identification of porphyry quartz based on cathodoluminescence (CL) and fluid inclusion characteristics.

that all dust was removed. After drying, the sample was split again using a riffle splitter. Two 15-g splits were transferred to 250-ml separatory funnels for density separation. Using lithium metatungstate—a variable density, heavy-liquid solution—rock and mineral grains having a density below 2.62 g \cdot cm $^{-3}$ and above 2.73 g \cdot cm $^{-3}$ were removed (quartz has a density of 2.68 g \cdot cm $^{-3}$). After density separation, the two sample splits were recombined and thoroughly washed to recover the lithium metatungstate.

The obtained density separates were then used to prepare grain mounts. Initially, a double-sided sticky tape was mounted on a glass slide. A 35-mm plastic mold was then placed on the tape. A thin layer of the grains was poured into the mold, avoiding clustering and overlapping of the grains. The mold was then backfilled with epoxy and cured for \sim 4 hours in a vacuum vessel to remove bubbles from the epoxy. Subsequently, a single, polished, 60-µm-thick section was prepared from each grain mount. The sample preparation methods detailed above, particularly selection of the 250- to 500-µm-size fractions, ensured that each thick section contained a minimum of \sim 1,000 sand grains, with some of the sections containing up to \sim 5,000 grains.

The thick sections were then carbon coated and inspected using a HC5-LM hot cathode CL microscope by Lumic Special Microscopes, Germany. The microscope was operated at 14 kV and with a current density of $\sim\!10~\mu\text{A}$ mm $^{-2}$ (Neuser, 1995). Quartz grains showing blue to purple CL emissions were identified by screening of the grain mounts and were marked on a scan of the thick section obtained at high resolution using a standard document scanner. Subsequently, fluid inclusion petrography was conducted on the quartz grains showing a blue to purple CL emission using an Olympus BX51 optical microscope. Based on the criteria established above (Fig. 2), quartz grains that were certainly derived from a porphyry, and those that possibly originated from a porphyry were identified and counted in each mount.

To determine the total number of sand grains in each sample, the high-resolution image of the thick section was con-

verted into a 1-bit black-and-white image and processed using thresholding and watershed segmentation techniques for automated counting (Sime and Ferguson, 2003) in the software program ImageJ. This preprocessing step of the images corrects for the effects of clustering and overlapping of the grains in the mounts and allows the program to reliably determine the total number of grains in each thick section. As a final step, the concentration of porphyry quartz grains observed was calculated relative to the total number of sand grains in the mount, such that concentrations between samples could be compared.

Dispersion Studies

Two dispersion studies were conducted to evaluate the applicability of the method developed using the coarse rejects of geochemically anomalous BLEG samples collected as part of a regional exploration program conducted by Newmont Corp. This included the study of eight stream sediment samples from Vert de Gris in Haiti that were collected within the catchment area of a known porphyry prospect. In addition, eight stream sediment samples were collected at Hides Creek in Papua New Guinea.

Vert de Gris, Haiti

The Vert de Gris porphyry Cu-Mo prospect is located on the northern peninsula of Haiti (Fig. 3; Arribas et al., 2017). The prospect is situated near the city Jean-Rabel, which is $\sim\!100~\rm km$ west of Cap-Haitien. Within the Vert de Gris area, a 6-km²-large erosional window through Eocene limestone exposes a mineralized Late Cretaceous intrusive complex that has been dated at 67.3 \pm 4 Ma (Cheilletz et al., 1978). The intrusive rocks include, from oldest to youngest, locally porphyritic hornblende-biotite tonalite, rhyodacite porphyry intrusions and intrusive breccias, and dikes of hornblende andesite porphyry. The mineralized zone consisting of bornite, chalcopyrite, and minor molybdenite is centered on the intrusions and is hosted in part within a rhyodacite breccia. Elevated base metal grades are associated with potassic alteration con-

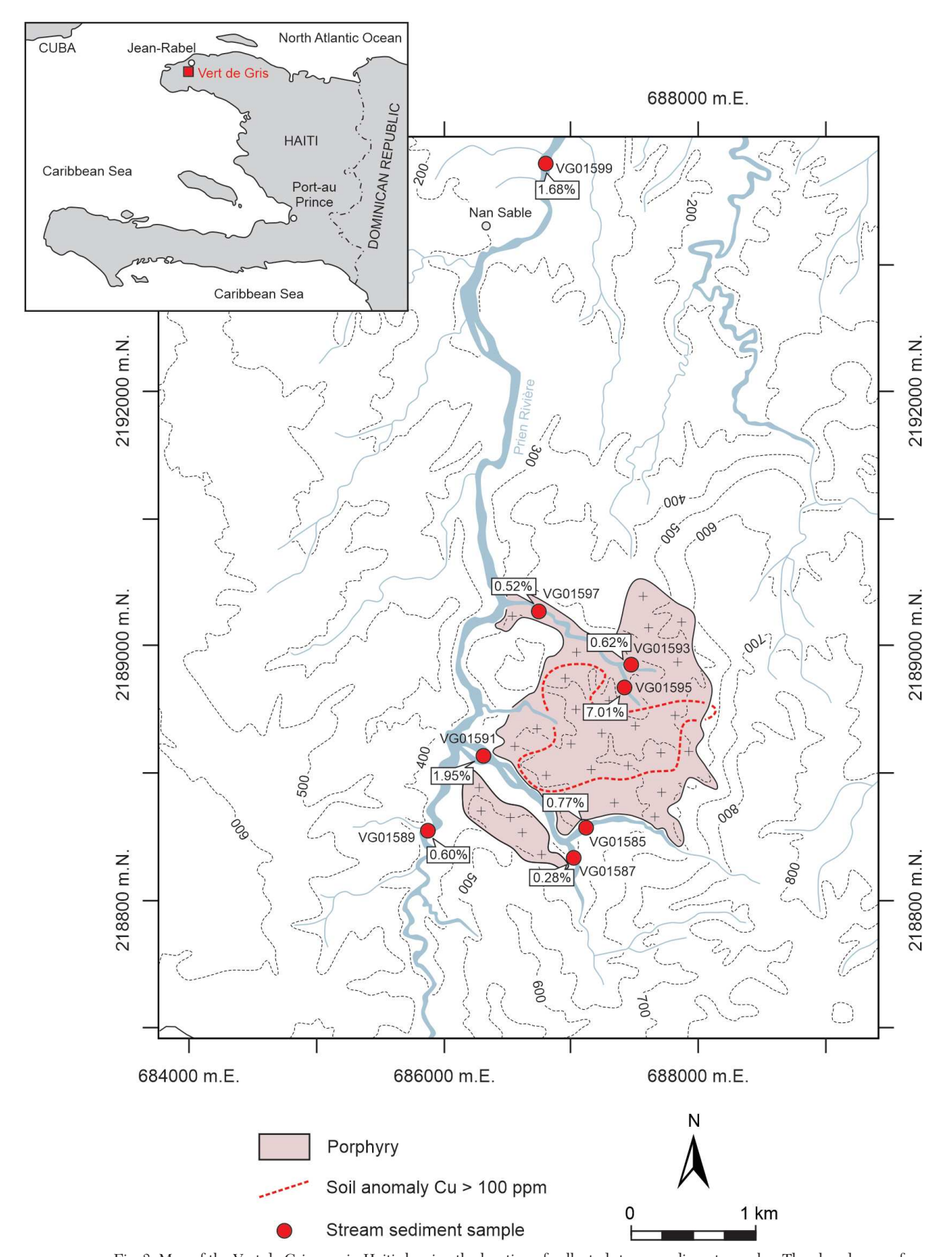


Fig. 3. Map of the Vert de Gris area in Haiti showing the location of collected stream sediment samples. The abundances of porphyry quartz grains are given in percentages (see Table 1). The map also displays the distribution of outcropping porphyritic rocks and the location of a soil geochemical anomaly. The contour intervals are given in meters above sea level.

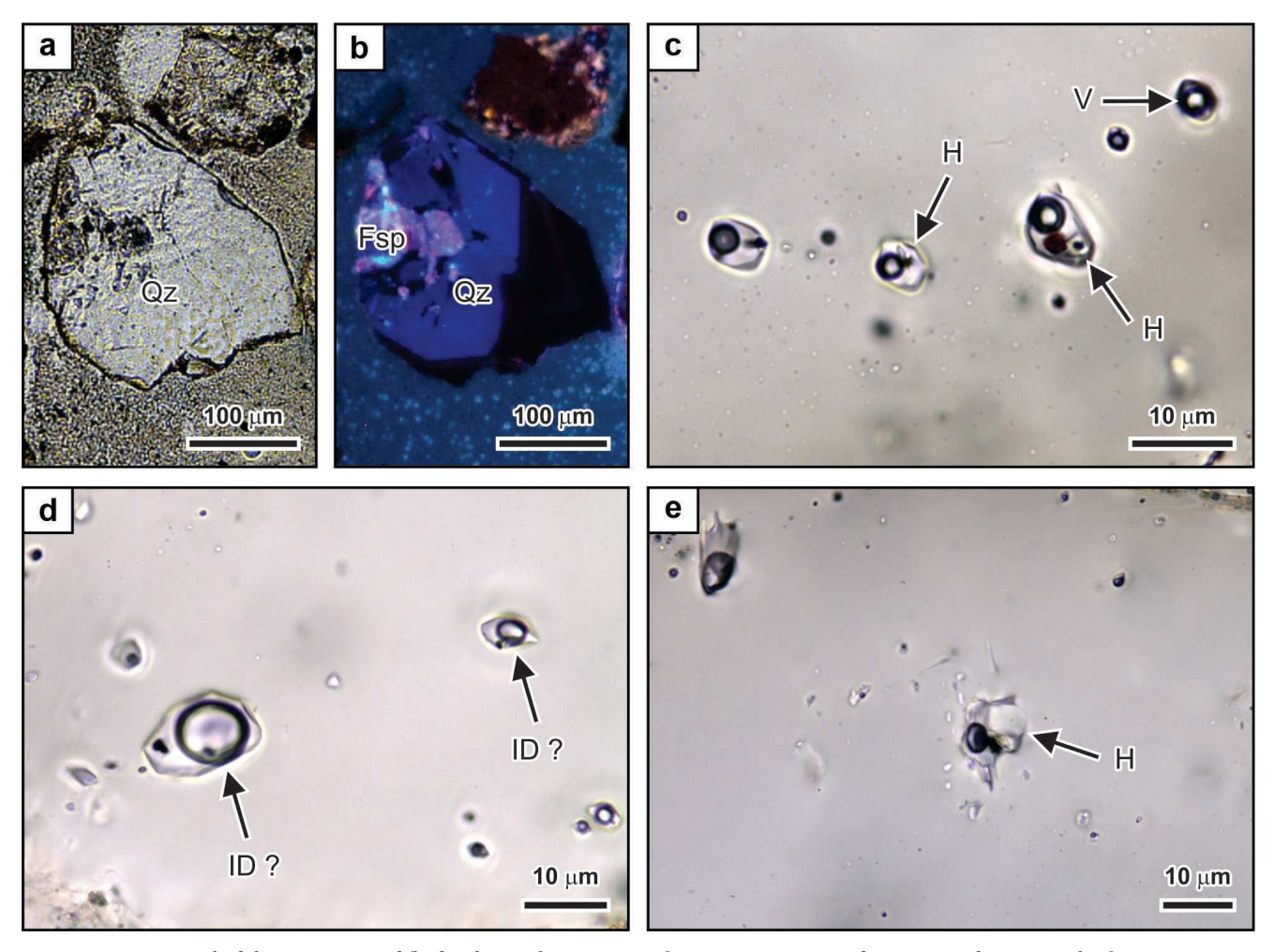


Fig. 4. Cathodoluminescence and fluid inclusion characteristics of quartz grains contained in stream sediment samples from the Vert de Gris area in Haiti. (a) Plane-polarized light image of a quartz grain hosting porphyry-type fluid inclusions. Sample VG01593. (b) Corresponding optical cathodoluminescence image showing that the quartz grain exhibits a long-lived blue emission. The quartz is intergrown with feldspar showing a pink to light blue cathodoluminescence emission. (c) Secondary, healed microfracture showing hypersaline liquid and vapor-rich fluid inclusions. Sample VG01587. (d) Possible intermediate-density fluid inclusions. Sample VG01595. (e) Hypersaline liquid inclusion surrounded by neonate inclusions, which is evidence for postentrapment modification. Sample VG01585. Abbreviations: Fsp = feldspar, H = hypersaline liquid fluid inclusion, ID? = possible intermediate-density fluid inclusion, Qz = quartz, V = vapor-rich fluid inclusion.

sisting of K-feldspar and secondary biotite. Later-stage phyllic alteration and a large propylitic alteration halo have been recognized (Cheilletz et al., 1978; Nelson et al., 2011).

The coarse rejects of eight geochemically anomalous BLEG stream sediment samples were available from early-phase exploration that were collected at different distances to the mineralized zone defined during later exploration work (Fig. 3). The samples contain abundant quartz grains that show a long-lived blue CL emission (Fig. 4a, b). The quartz grains typically are homogeneous in CL although some grains exhibiting growth zoning are present. In all samples, at least half of the quartz with a blue emission is overprinted along fractures by quartz with red-brown luminescence. For samples VG01585 and VG01591, the number of quartz grains having a blue CL with overprinting red-brown CL is almost twice that of grains with a blue CL color alone. Quartz grains with a blue luminescence can be intergrown with K-feldspar that shows a bright pink or light blue luminescence (Fig. 4b). These grains may

represent hydrothermally altered quartz phenocrysts or are derived from thin veins surrounded by wall rocks.

The quartz grains showing a blue CL emission typically contain randomly oriented and closely spaced healed microfractures of hypersaline liquid inclusions containing halite crystals (Fig. 4c). The hypersaline liquid inclusions range in shape from irregular to negative crystal shaped. The volumetric proportions of the vapor bubbles and halite crystals are variable. In some cases, the hypersaline liquid inclusions contain daughter crystals including opaque phases. Some of the quartz grains containing hypersaline liquid inclusions also host vapor-rich inclusions (Fig. 4c), although some quartz grains host vaporrich inclusions only. Some quartz grains contain possible intermediate-density inclusions (Fig. 4d), which may contain small opaque daughter minerals. In some cases, the porphyry quartz grains are crosscut by trails of liquid-rich inclusions. These are particularly common in grains that have been overprinted by zones of red-brown luminescence. Some high-salinity inclusions (Fig. 4e) and intermediate-density inclusions show textures suggestive of postentrapment modification.

The dispersion study at Vert de Gris shows that the number of porphyry quartz grains— identified using the criteria summarized in Figure 2—in the eight stream sediment samples can be used for targeting (Table 1). Sample VG01587, collected at the southern margin of the target area (Fig. 3), contained the lowest number of porphyry quartz grains, with porphyry quartz making up 0.28% of the grains in the mount. Only two grains in the sample were confidently identified as being derived from a porphyry source (Table 1). Samples VG01585, VG01589, and VG01597, located along the margins of the target area, show similarly low concentrations of porphyry grains, ranging from 0.52 to 0.77%. However, these samples contained a higher proportion of confidently identified porphyry grains (Table 1). The concentration of porphyry quartz grains is higher downstream of an area of anomalous soil geochemistry (Fig. 3). Sample VG01591 taken at this location contained 1.95% porphyry quartz grains. A high concentration of 7.01% porphyry quartz grains was encountered in sample VG01595, collected near the center of the target area. This sample contained the highest count—27 certain porphyry quartz grains (Table 1). Sample VG01593, collected adjacent to and at approximately the same elevation, contained a comparatively lower concentration of 0.62% porphyry quartz grains. Sample VG01599 had a 1.68% concentration of porphyry quartz grains, despite being located ~3.5 km downstream of the target area (Fig. 3).

Hides Creek, Papua New Guinea

The Hides Creek porphyry prospect is in the southeastern Morobe district of Papua New Guinea (Fig. 5; Arribas et al., 2017). The Morobe district is host to several major precious metal deposits that have been associated with porphyry intrusions, including the Wau Au deposit (Sillitoe et al., 1984; Carswell, 1990), the Hidden Valley Au-Ag deposit (Nelson et al., 1990), and the Golpu porphyry Cu-Au and associated Wafi high- and intermediate-sulfidation epithermal Au deposits (Rinne et al., 2018).

Basement rocks within the Morobe district include metasedimentary deposits of the Early Cretaceous Owen Stanley Formation (Sillitoe et al., 1984; Rinne et al., 2018). These were overthrust by an ophiolite suite at ~60 Ma (Lus et al., 2004). Subsequent metamorphism resulted in a greenschist facies overprint of the basement rocks (Davies and Williamson, 2001). In the central part of the Morobe district, the basement is intruded by the 14.5 to 12 Ma Morobe granodiorite, which represents a composite intrusion consisting of granodiorite, diorite, and monzonite (Tingey and Grainger, 1976). The intrusive center at Wafi-Golpu has been dated at 8.76 ± 0.02 and 8.73 ± 0.01 Ma (Rinne et al., 2018). The youngest igneous rocks in the area include the Pliocene Bulolo volcanic rocks, consisting of several hundred meters of poorly bedded felsic ignimbrite, and comagmatic intrusions (Rinne et al., 2018). Broadly contemporaneous to the Bulolo volcanic rocks is the Pliocene Otibanda Formation, which forms a several-hundred-meters-thick lacustrine to fluvial succession of interbedded sandstone, conglomerate, tuff, and limestone (Page and McDougall, 1972; Sillitoe et al., 1984).

The coarse rejects of eight geochemically anomalous BLEG samples from Hides Creek were obtained for this study (Fig. 5). The stream sediment samples contain only a few quartz grains with a blue CL color (Fig. 6a). Most quartz grains exhibit a homogeneous CL, although grains showing oscillatory growth zoning have been observed (Fig. 6b). Overprint of the quartz with a blue emission by zones of redbrown luminescence was observed in samples HC66311 (Fig. 6a), HC66312, HC66315, and HC66317. Many of the quartz grains showing a blue CL emission contain arrays of healed microfractures of hypersaline liquid and vapor-rich fluid inclusions (Fig. 6c). The volumetric proportions of the vapor bubbles and halite crystal are variable, and other daughter phases are present. Many of the quartz grains exhibiting a blue CL color also contain possible intermediate-density fluid inclusions (Fig. 6d). Hypersaline and intermediate density inclusions commonly show textures indicative of postentrapment modification (Fig 6e).

The stream sediments collected at Hides Creek show low percentages of porphyry quartz grains (Table 2) based on the established CL and fluid inclusion criteria (Fig. 2). The highest concentrations of porphyry quartz were encountered in two samples located within ~1.5 km from the target area. Samples HC66315 and HC66317 contained 0.66 and 0.31% porphyry quartz, respectively (Table 2). Concentrations of porphyry quartz grains decrease further down the drainage pattern to 0.05 to 0.07% in samples HC66312 and HC66311 (Table 2). Samples HC66313 and HC66318, located along a different drainage fork from the target area, lacked porphyry quartz grains. No porphyry quartz grains were identified in samples HC66314 and HC66316 (Table 2) despite their proximity to the target area and high BLEG values of 40.6 and

Table 1. Summary of Stream Sediment Characteristics from the Vert de Gris Area, Haiti

Sample	Total number of grains in mount	Number of certain porphyry quartz grains	Number of possible porphyry quartz grains	Abundance of porphyry quartz grains (%)
VG01585	4,388	5	29	0.77
VG01587	2,891	2	6	0.28
VG01589	2,827	3	14	0.60
VG01591	1,694	9	24	1.95
VG01593	3,227	2	18	0.62
VG01595	1,112	27	51	7.01
VG01597	4,815	2	23	0.52
VG01599	1,843	7	24	1.68

Note: Criteria used to identify porphyry quartz grains and to distinguish between grains of certain and possible porphyry origin are summarized in Figure 2

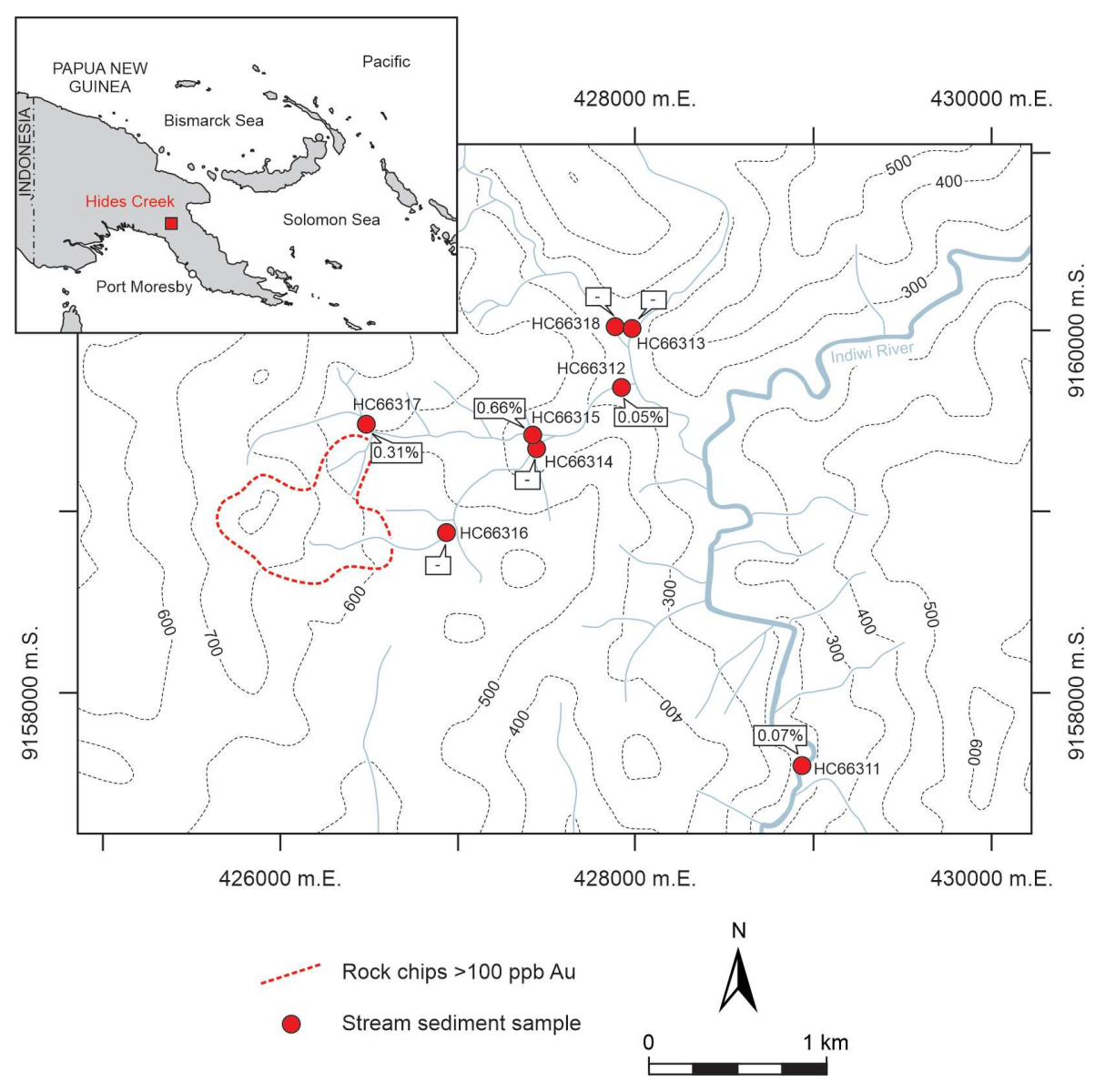


Fig. 5. Map of the Hides Creek area in Papua New Guinea showing the location of stream sediment samples collected. The abundances of porphyry quartz grains are given in percentages (see Table 2). The map also displays the distribution of rock chip samples returning elevated Au concentrations. The contour intervals are given in meters above sea level. Note: "-" = not detected.

71 ppb Au, respectively. Follow-up field work showed that the sample HC66316 was taken close to an outcrop of a quartz vein interpreted to be a low-sulfidation epithermal vein. This suggests that the method developed may be effective in identifying complexities of stream sediment geochemical anomalies caused by different styles of mineralization.

Potential Applications in Mineral Exploration

The case studies conducted at Vert de Gris and Hides Creek demonstrate that porphyry quartz grains can be successfully identified in stream sediment samples at low concentrations using the microscopic methods described and that quantification of the abundance of these grains is possible. Because porphyry quartz grains were dispersed up to several kilometers away from the inferred source, quartz can be used as an indicator mineral to locate eroding porphyries within the sampled catchment areas. The two case studies provide proof of concept that the developed method is viable.

It is envisaged that the method described here can be most effectively implemented in greenfield exploration programs that aim to identify porphyry targets through BLEG stream sediment surveys at district or even country scales. In regional geochemical surveys, several hundred to thousand BLEG stream sediment samples are collected across large swaths of land at an average density of one sample per several square kilometers (Carlile et al., 1998; Leduc and Itard, 2003; Yilmaz et al., 2017). Following geochemical analysis of these samples, infill samples are collected to increase sample coverage in areas regarded to be favorable. Based on the results of the geochemical analyses of these infill samples, targets are de-

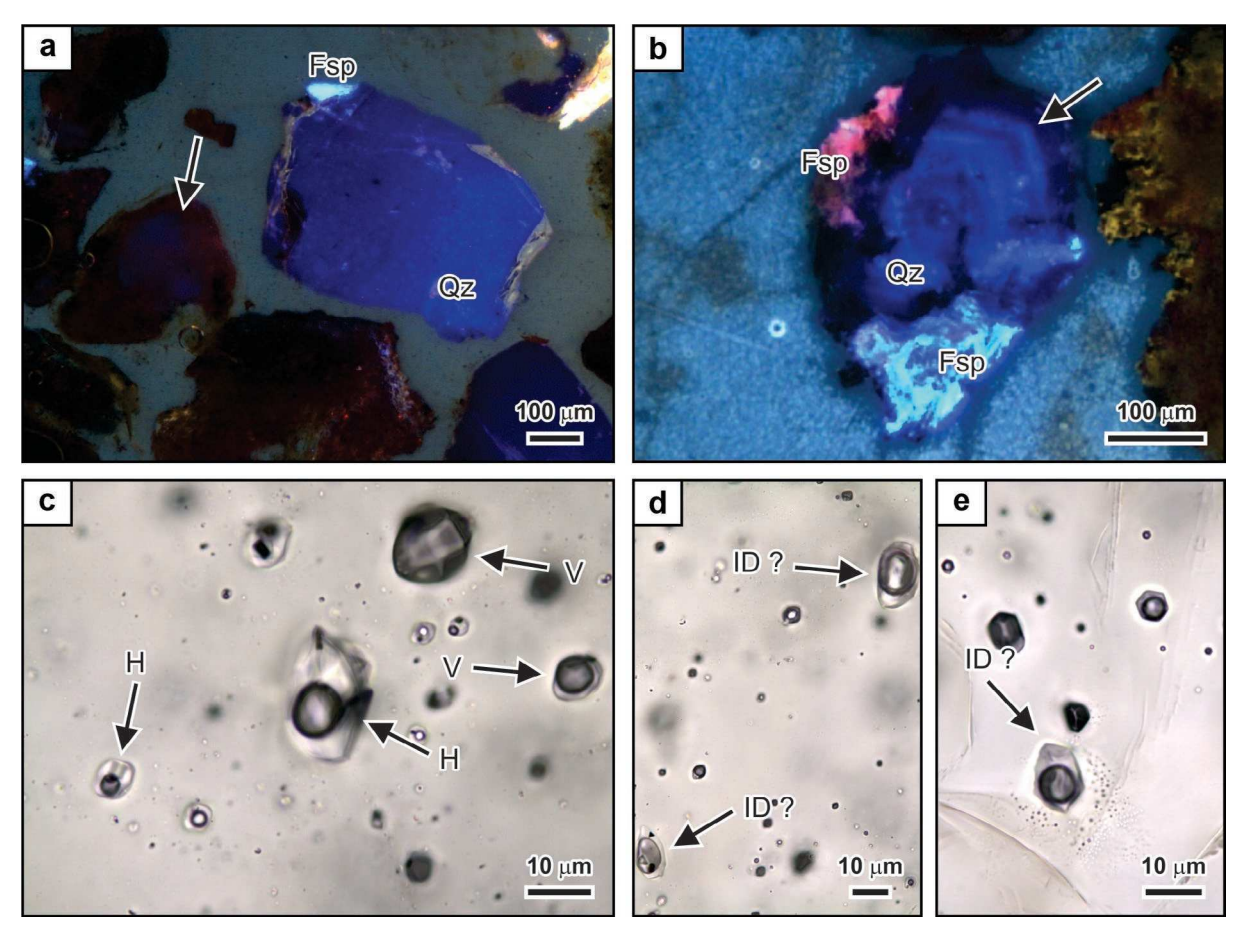


Fig. 6. Cathodoluminescence and fluid inclusion characteristics of quartz grains contained in stream sediment samples from the Hides Creek area in Papua New Guinea. (a) Quartz grain showing homogeneous, long-lived blue cathodoluminescence emission. An early blue quartz grain overprinted by dull red quartz is visible in the same field of view (arrow). Sample HC66311. (b) Bright blue luminescent quartz grain with well-developed oscillatory growth zoning (arrow). The grain is intergrown with feldspar. Sample HC66317. (c) Hypersaline liquid inclusions and vapor-rich fluid inclusions. Sample HC66315. (d) Possible intermediate-density fluid inclusions. The inclusion on the lower left side contains a probable chalcopyrite daughter crystal. Sample HC66315. (e) Possible intermediate-density fluid inclusions surrounded by a halo of satellite neonate inclusions, which provide evidence for postentrapment modification. Sample HC66311. Abbreviations: Fsp = feldspar, H = hypersaline liquid fluid inclusion, ID ? = possible intermediate-density fluid inclusion, Qz = quartz, V = vapor-rich fluid inclusion.

Table 2. Summary of Stream Sediment Characteristics from the Hides Creek Area, Papua New Guinea

Sample	Total number of grains in mount	Number of certain porphyry quartz grains	Number of possible porphyry quartz grains	Abundance of porphyry quartz grains (%)
HC66311	4,457	0	3	0.07
HC66312	3,918	2	0	0.05
HC66313	2,664	0	0	-
HC66314	3,828	0	0	-
HC66315	1,959	3	10	0.66
HC66316	1,974	0	0	-
HC66317	1,951	1	5	0.31
HC66318	3,918	0	0	-

Notes: Criteria used to identify porphyry quartz grains and to distinguish between grains of certain and possible porphyry origin are summarized in Figure 2; "-" indicates not detected

lineated that will be followed up on by mapping, geophysical surveys, or drilling.

In large, regional exploration programs, it is critical to objectively prioritize targets for more expensive follow-up work. It is suggested here that the porphyry quartz content of the

stream sediments can be used as a ranking criterion to differentiate porphyry-related BLEG anomalies from nonporphyry-related targets following geochemical analysis. Analogous to the present study, the optical CL and fluid inclusion investigation could be conducted on the coarse rejects of BLEG samples already analyzed geochemically. Because only samples returning anomalous geochemical results would be of interest, only a subset of the total number of stream sediment samples collected in the regional or country-wide survey would need to be analyzed using the methods described in this contribution. Selecting a reduced subset of samples for examination will make the use of the petrographic methods described here economically feasible enough to allow implementation into exploration workflows. The information gained may be valuable enough to justify the additional analytical expense, especially given the fact that original sample collection in the field represents a significant cost factor.

Measuring the abundance of porphyry quartz grains in stream sediments will provide an important ranking criterion for prospects with anomalous BLEG geochemical characteristics. The case studies at Vert de Gris and Hides Creek, where known porphyry occurrences are in the catchment areas, showed that porphyry quartz grains can be confidently identified using the established criteria (Fig. 2).

Limitations and Areas for Future Improvement

It is important to note that the method presented in this contribution was developed to target porphyry deposits formed at intermediate crustal depths where high-temperature quartz contains hypersaline liquid and vapor-rich inclusions (Monecke et al., 2018). High-temperature quartz sourced from an eroding porphyry deposit associated with a deep (≥4.2 km) intrusion may be more challenging to identify because intermediate-density fluid inclusions would be prevalent, which are difficult to distinguish in grain mounts from quartz from other geologic environments even if inspected by an experienced fluid inclusionist. Therefore, deep porphyry deposits such as Butte in Montana (Rusk et al., 2008) may not be readily identified using the method proposed here. Knowledge of the erosional level in the exploration area may be critical to ensure that such deep systems are not overlooked by overinterpreting the information that can be obtained from quartz analysis.

Integration of the techniques proposed in this contribution into large greenfield exploration programs may require further streamlining of the analytical procedure to reduce personnel time and cost for consumables. Under routine conditions, it appears feasible that the second step of heavy-mineral separation—removing minerals having a density exceeding 2.72 g · cm⁻³—could be replaced or supplemented by magnetic separation using a Frantz magnetic separator to further enhance the amount of quartz that is recovered. Further systematic tests may be required to optimize the sample preparation procedure for stream sediments of different mineralogical composition, which could be the case if different rock types are exposed in the sampled catchment areas.

Acknowledgments

Antonio Arribas suggested the research topic, arranged for partial funding from Newmont Corp., and selected and organized the pilot studies in Haiti and Papua New Guinea. We are indebted to Mike Belperio, Mark Lindsay, Daven Mashburn, Nigel Radford, and the rest of the Newmont Haiti and Papua New Guinea exploration teams for organizing the stream sediment sampling and providing the results of the BLEG surveys. Matthew Dye, Katharina Pfaff, Carla

Sanchez, and the late John Skok at Colorado School of Mines are thanked for analytical support and assistance in making the grain mounts. We acknowledge Michael Schmid at the University of Vienna in Austria for the development of the thresholding and watershed segmentation plug-in for ImageJ used for grain counting. Financial support for the research was provided by Newmont Corp. Additional financial support was provided by the Society of Economic Geologists and Colorado School of Mines to M.M.B. We acknowledge José Perelló and Katie McFall for their constructive reviews of an earlier version of this contribution.

REFERENCES

Arribas, A., Bennett, M., Monecke, T., Reynolds, J., and Kelly, N., 2017, Early-stage porphyry Cu-Au exploration: Adding value to regional stream sediment surveys by studying fluid inclusions [ext. abs.]: FUTORES II (Future Understanding of Tectonics, Ores, Resources, Environment and Sustainability), Townsville, Australia, EGRU (Economic Geology Research Centre) Contribution, v. 69, p. 3.

Augustsson, C., and Reker, A., 2012, Cathodoluminescence spectra of quartz as provenance indicators revisited: Journal of Sedimentary Research, v. 82, p. 559–570.

Blatt, H., 1987, Oxygen isotopes and the origin of quartz: Journal of Sedimentary Petrology, v. 57, p. 373–377.

Bodnar, R.J., 1995, Fluid-inclusion evidence for a magmatic source for metals in porphyry copper deposits: Mineralogical Association of Canada, Short Course 23, p. 139–152.

Bodnar, R.J., Lecumberri-Sanchez, P., Moncada, D., and Steele-MacInnis, M., 2014, Fluid inclusions in hydrothermal ore deposits, *in* Holland, H.D., and Turekian, K.K., eds., Treatise on geochemistry, v. 13, 2nd ed.: Oxford, Elsevier, p. 119–142.

Bottrell, S.H., Yardley, B., and Buckley, F., 1988, A modified crush-leach method for the analysis of fluid inclusion electrolytes: Bulletin de Minéralogie, v. 111, p. 279–290.

Carlile, J.C., Davey, G.R., Kadir, I., Langmead, R.P., and Rafferty, W.J., 1998, Discovery and exploration of the Gosowong epithermal gold deposit, Halmahera, Indonesia: Journal of Geochemical Exploration, v. 60, p. 207–227.

Carswell, J.T., 1990, Wau gold deposits, in Hughes, F.E., ed., Geology of the mineral deposits of Australia and Papua New Guinea: Melbourne, Australasian Institute of Mining and Metallurgy, v. 2, p. 1763–1767.

Chang, J., Li, J.W., and Audétat, A., 2018, Formation and evolution of multistage magmatic-hydrothermal fluids at the Yulong porphyry Cu-Mo deposit, eastern Tibet: Insights from LA-ICP-MS analysis of fluid inclusions: Geochimica et Cosmochimica Acta, v. 232, p. 181–205.

Cheilletz, A., Kachrillo, J.J., Sonet, J., and Zimmerman, J.L., 1978, Pétrographie et géochronologie de deux complexes intrusifs à porphyres cuprifères d'Haïti, Contribution à la connaissance de la province cuprifère laramienne de l'arc insulaire de Grandes Antilles: Bulletin de la Societé Géologique de France, v. 20, p. 907–914.

Clayton, R.N., Rex, R.W., Syers, J.K., and Jackson, M.L., 1972, Oxygen isotope abundance in quartz from Pacific pelagic sediments: Journal of Geophysical Research, v. 77, p. 3907–3915.

Davies, H.L., and Williamson, A.N., 2001, Explanatory notes to accompany Buna 1:250,000 geological map: Geological Survey of Papua New Guinea, p. 1–23.

Dilles, J.H., and Einaudi, M.T., 1992, Wall-rock alteration and hydrothermal flow paths about the Ann-Mason porphyry copper deposit, Nevada—a 6-km vertical reconstruction: Economic Geology, v. 87, p. 1963–2001.

Fournier, R.O., 1967, The porphyry copper deposit exposed in the Liberty open-pit mine near Ely, Nevada, Part I, Syngenetic formation: Economic Geology, v. 62, p. 57–81.

Gao, S., Zou, X., Hofstra, A.H., Qin, K., Marsh, E.E., Bennett, M.M., Li, G., Jiang, J., Su, S., Zhao, J., and Li, Z., 2022, Trace elements in quartz: Insights into source and fluid evolution in magmatic-hydrothermal systems: Economic Geology, v. 117, p. 1415–1428.

Götze, J., Plötze, M., and Habermann, D., 2001, Origin, spectral characteristics and practical applications of the cathodoluminescence (CL) of quartz—a review: Mineralogy and Petrology, v. 71, p. 225–250.

Götze, J., Plötze, M., Graupner, T., Hallbauer, D.K., and Bray, C.J., 2004, Trace element incorporation into quartz: A combined study by ICP-MS,

- electron spin resonance, cathodoluminescence, capillary ion analysis, and gas chromatography: Geochimica et Cosmochimica Acta, v. 68, p. 3741–3759.
- Gregory, M.J., 2017, A fluid inclusion and stable isotope study of the Pebble porphyry copper-gold-molybdenum deposit, Alaska: Ore Geology Reviews, v. 80, p. 1279–1303.
- Gruen, G., Heinrich, C.A., and Schroeder, K., 2010, The Bingham Canyon porphyry Cu-Mo-Au deposit, II, Vein geometry and ore shell formation by pressure-driven rock extension: Economic Geology, v. 105, p. 69–90.
- Gustafson, L.B., and Hunt, J.P., 1975, The porphyry copper deposit at El Salvador, Chile: Economic Geology, v. 70, p. 857–912.
- Gustafson, L.B., and Quiroga, J., 1995, Patterns of mineralization and alteration below the porphyry copper orebody at El Salvador, Chile: Economic Geology, v. 90, p. 2–16.
- Hedenquist, J.W., Arribas, Jr., A., and Reynolds, T.J., 1998, Evolution of an intrusion-centered hydrothermal system: Far Southeast-Lepanto porphyry and epithermal Cu-Au deposits, Philippines: Economic Geology, v. 93, p. 373–404.
- Heinrich, C.A., Günther, D., Audétat, A., Ulrich, T., and Frischknecht, R., 1999, Metal fractionation between magmatic brine and vapor, determined by microanalysis of fluid inclusions: Geology, v. 27, p. 755–758.
- Heynke, U., Leeder, O., and Schulz, H., 1992, On distinguishing quartz of hydrothermal or metamorphogenic origin in different monomineralic veins in the eastern part of Germany: Mineralogy and Petrology, v. 46, p. 315–329.
- Hezarkhani, A., and Williams-Jones, A.E., 1998, Controls of alteration and mineralization in the Sungun porphyry copper deposit, Iran: Evidence from fluid inclusions and stable isotopes: Economic Geology, v. 93, p. 651–670.
- İmer, A., Richards, J.P., and Muehlenbachs, K., 2016, Hydrothermal evolution of the Cöpler porphyry-epithermal Au deposit, Erzincan Province, central eastern Turkey: Economic Geology, v. 111, p. 1619–1658.
- Klemm, L.M., Pettke, T., Heinrich, C.A., and Campos, E., 2007, Hydrothermal evolution of the El Teniente deposit, Chile: Porphyry Cu-Mo ore deposition from low-salinity magmatic fluids: Economic Geology, v. 102, p. 1021–1045
- Klyukin, Y.I., Steele-MacInnis, M., Lecumberri-Sanchez, P., and Bodnar, R.J., 2019, Fluid inclusion phase ratios, compositions and densities from ambient temperature to homogenization, based on PVTX properties of H₂O-NaCl: Earth-Science Reviews, v. 198, article 102924.
- Landtwing, M.R., Furrer, C., Redmond, P.B., Pettke, T., Guillong, M., and Heinrich, C.A., 2010, The Bingham Canyon porphyry Cu-Mo-Au deposit, III, Zoned copper-gold ore deposition by magmatic vapor expansion: Economic Geology, v. 105, p. 91–118.
- Leduc, C., and Itard, Y., 2003, Low sampling density exploration geochemistry for gold in arid and tropical climates: Comparison between conventional geochemistry and BLEG: Geochemistry: Exploration, Environment, Analysis, v. 3, p. 121–131.
- Lowell, J.D., and Guilbert, J.M., 1970, Lateral and vertical alteration-mineralization zoning in porphyry ore deposits: Economic Geology, v. 65, p. 373–408.
- Lus, W.Y., McDougall, I., and Davies, H.L., 2004, Age of the metamorphic sole of the Papuan ultramafic belt ophiolite, Papua New Guinea: Tectonophysics, v. 392, p. 85–101.
- Maryono, A., Harrison, R.L., Cooke, D.R., Rompo, I., and Hoschke, T.G., 2018, Tectonics and geology of porphyry Cu-Au deposits along the eastern Sunda magmatic arc, Indonesia: Economic Geology, v. 113, p. 7–38.
- Meldrum, S.J., Aquino, R.S., Gonzales, R.I., Burke, R.J., Suyadi, A., Irianto, B., and Clarke, D.S., 1994, The Batu Hijau porphyry copper-gold deposit, Sumbawa Island, Indonesia: Journal of Geochemical Exploration, v. 50, p. 203–220
- Monecke, T., Kempe, U., and Götze, J., 2002, Genetic significance of the trace element content in metamorphic and hydrothermal quartz: A reconnaissance study: Earth and Planetary Science Letters, v. 202, p. 709–724.
- Monecke, T., Monecke, J., Reynolds, T.J., Tsuruoka, S., Bennett, M.M., Skewes, W.B., and Palin, R.M., 2018, Quartz solubility in the H₂O-NaCl system: A framework for understanding vein formation in porphyry copper deposits: Economic Geology, v. 113, p. 1007–1046.
- Müller, A., Herrington, R., Armstrong, R., Seltmann, R., Kirwin, D.J., Stenina, N.G., and Kronz, A., 2010, Trace elements and cathodoluminescence of quartz in stockwork veins of Mongolian porphyry-style deposits: Mineralium Deposita, v. 45, p. 707–727.
- Nelson, C.E., Proenza, J.A., Lewis, J.F., and López-Kramer, J., 2011, The metallogenic evolution of the Greater Antilles: Geologica Acta, v. 9, p. 229–264.

- Nelson, R.W., Bartram, J.A., and Christie, M.H., 1990, Hidden Valley gold-silver deposit, *in* Hughes, F.E., ed., Geology of the mineral deposits of Australia and Papua New Guinea: Melbourne, Australasian Institute of Mining and Metallurgy, p. 1773–1776.
- Neuser, R.D., 1995, A new high-intensity cathodoluminescence microscope and its application to weakly luminescing minerals: Bochumer Geologische und Geotechnische Arbeiten, v. 44, p. 116–118.
- Nielsen, R.L., 1968, Hypogene texture and mineral zoning in a copper-bearing granodiorite porphyry stock, Santa Rita, New Mexico: Economic Geology, v. 63, p. 37–50.
- Page, R.W., and McDougall, I., 1972, Ages of mineralization of gold and porphyry copper deposits in the New Guinea highlands: Economic Geology, v. 67, p. 1034–1048.
- Palmer, S.E., Kyser, T.K., and Hiatt, E.E., 2004, Provenance of the Proterozoic Thelon basin, Nunavut, Canada, from detrital zircon geochronology and detrital quartz oxygen isotopes: Precambrian Research, v. 129, p. 115–140.
- Perelló, J., Razique, A., Schloderer, J., and Rehman, A., 2008, The Chagai porphyry copper belt, Baluchistan province, Pakistan: Economic Geology, v. 103, p. 1583–1612.
- Pudack, C., Halter, W.E., Heinrich, C.A., and Pettke, T., 2009, Evolution of magmatic vapor to gold-rich epithermal liquid: The porphyry to epithermal transition at Nevados de Famatina, northwest Argentina: Economic Geology, v. 104, p. 449–477.
- Redmond, P.B., Einaudi, M.T., Inan, E.E., Landtwing, M.R., and Heinrich, C.A., 2004, Copper deposition by fluid cooling in intrusion-centered systems: New insights from the Bingham porphyry ore deposit, Utah: Geology, v. 32, p. 217–220.
- Reynolds, T.J., and Beane, R.E., 1985, Evolution of hydrothermal fluid characteristics at the Santa Rita, New Mexico, porphyry copper deposit: Economic Geology, v. 80, p. 1328–1347.
- Richards, J.P., 2011, Magmatic to hydrothermal metal fluxes in convergent and collided margins: Ore Geology Reviews, v. 40, p. 1–26.
- Rinne, M.L., Cooke, D.R., Harris, A.C., Finn, D.J., Allen, C.M., Heizler, M.T., and Creaser, R.A., 2018, Geology and geochronology of the Golpu porphyry and Wafi epithermal deposit, Morobe Province, Papua New Guinea: Economic Geology, v. 113, p. 271–294.
- Rusk, B., 2012, Cathodoluminescent textures and trace elements in hydrothermal quartz, in Götze, J., and Möckel, R., eds., Quartz: Deposits, mineralogy and analytics: Berlin, Springer, p. 307–329.
 Rusk, B.G., Reed, M.H., and Dilles, J.H., 2008, Fluid inclusion evidence for
- Rusk, B.G., Reed, M.H., and Dilles, J.H., 2008, Fluid inclusion evidence for magmatic-hydrothermal fluid evolution in the porphyry copper-molybdenum deposit at Butte, Montana: Economic Geology, v. 103, p. 307–334.
- Seedorff, E., Dilles, J.H., Proffett, Jr., J.M., Einaudi, M.T., Zurcher, L., Stavast, W.J.A., Johnson, D.A., and Barton, M.D., 2005, Porphyry deposits: Characteristics and origin of hypogene features: Economic Geology 100th Anniversary Volume, p. 251–298.
- Sillitoe, R.H., 2010, Porphyry copper systems: Economic Geology, v. 105, p. 3–41
- Sillitoe, R.H., and Thompson, J.F.H., 2006, Changes in mineral exploration practice: Consequences for discovery: Society of Economic Geologists Special Publication, v. 12, p. 193–219.
- Sillitoe, R.H., Baker, M.E., and Brook, W.A., 1984, Gold deposits and hydrothermal eruption breccias associated with a maar volcano at Wau, Papua New Guinea: Economic Geology, v. 79, p. 638–655.
- Sime, L.C., and Ferguson, R.I., 2003, Information on grain sizes in gravelbed rivers by automated image analysis: Journal of Sedimentary Research, v. 73, p. 630–636.
- Stefanova, E., Driesner, T., Zajacz, Z., Heinrich, C.A., Petrov, P., and Vasilev, Z., 2014, Melt and fluid inclusions in hydrothermal veins: The magmatic to hydrothermal evolution of the Elatsite porphyry Cu-Au deposit, Bulgaria: Economic Geology, v. 109, p. 1359–1381.
- Sun, M., Monecke, T., Reynolds, T.J., and Yang, Z., 2021, Understanding the evolution of magmatic-hydrothermal systems based on microtextural relationships, fluid inclusion petrography, and quartz solubility constraints: Insights into the formation of the Yulong Cu-Mo porphyry deposit, eastern Tibetan Plateau, China: Mineralium Deposita, v. 56, p. 823–842.
- Suttner, L.J., and Leininger, R.K., 1972, Comparison of the trace element content of plutonic, volcanic, and metamorphic quartz from southwestern Montana: Geological Society of America Bulletin, v. 83, p. 1855–1862.
- Tate, N.M., 2005, Discovery, geology and mineralisation of the Phu Kham copper-gold deposit Lao People's Democratic Republic [ext. abs.]: Deposit research: Meeting the global challenge. Eighth Biennial Society for

- Geology Applied to Mineral Deposits (SGA) Meeting, Beijing, China, 2005, Proceedings, p. 1077-1080.
- Tingey, R.J., and Grainger, O.J., 1976, Markham 1:250,000 geological map and exploratory notes: Papua New Guinea Geological Survey, sheet SB/55-10. Titley, S.R., and Beane, R.E., 1981, Porphyry copper deposits: Economic
- Geology 75th Anniversary Volume, p. 214–269.
- Tsuruoka, S., Monecke, T., and Reynolds, T.J., 2021, Evolution of the magmatic-hydrothermal system at the Santa Rita porphyry Cu deposit, New Mexico, USA: Importance of intermediate-density fluids in ore formation: Economic Geology, v. 116, p. 1267-1284.
- Ulrich, T., Günther, D., and Heinrich, C.A., 2002, The evolution of a porphyry Cu-Au deposit, based on LA-ICP-MS analysis of fluid inclusions: Bajo de la Alumbrera, Argentina: Economic Geology, v. 97, p. 1889–1920.
- Vennemann, T.W., Kesler, S.E., and O'Neil, J.R., 1992, Stable isotope compositions of quartz pebbles and their fluid inclusions as tracers of sediment provenance: Implications for gold- and uranium-bearing quartz pebble conglomerates: Geology, v. 20, p. 837–840.
- Watt, G.R., Wright, P., Galloway, S., and McLean, C., 1997, Cathodoluminescence and trace element zoning in quartz phenocrysts and xenocrysts: Geochimica et Cosmochimica Acta, v. 61, p. 4337–4348.
- Yardley, B.W.D., Banks, D.A., Bottrell, S.H., and Diamond, L.W., 1993, Postmetamorphic gold-quartz veins from N.W. Italy: The composition and origin of the ore fluid: Mineralogical Magazine, v. 57, p. 407–422.
- Yilmaz, H., Cohen, D.R., and Sonmez, F.N., 2017, Comparison between the effectiveness of regional BLEG and -80# stream sediment geochemistry in detection of precious and base metal mineral deposits in western Turkey: Journal of Geochemical Exploration, v. 181, p. 69–80.

Mitchell Bennett is a geologist at the U.S. Geological Survey in Denver, Colorado, where he performs fluid and melt inclusion analyses on a wide variety of forming systems, including orogenic Au, porphyry Cu, iron oxide copper-gold deposits, and rare earth element-bearing carbonatites. He also contributes to model-driven assessments for critical



mineral resources. He received a M.Sc. degree from the Colorado School of Mines in 2014, where he studied the characteristics of quartz occurring in porphyry veins. His areas of expertise include fluid inclusion petrography, microthermometry, cathodoluminescence microscopy, laser Raman spectroscopy, economic geology, critical mineral resources, and geothermal systems.